International Journal of Horticultural Science and Technology (2025) Vol. 12, No. 2, pp. 439-452 doi.org/10.22059/ijhst.2024.379984.893

International Journal of Horticultural Science and Technology
Journal homepage: https://ijhst.ut.ac.ir

Habitat Suitability Mapping on Significant Differences Between *Lolium perenne* and *L. rigidum*

Somayeh Esmaeili[1,2]*, Hassan Salehi[1]*, Morteza Khosh-Khui[1], Seyed Rashid Fallah Shamsi[3], Ali Reza Mikaeili Tabrizi[4], Mingying Xiang[5]

1 Department of Horticultural Science, School of Agriculture, Shiraz University, Shiraz, Iran
2 Department of Horticultural Science, Faculty of Agriculture, Shahid Chamran University of Ahvaz, Ahvaz, Iran
3 Department of Natural Resources and Environmental Engineering, School of Agriculture, Shiraz University, Shiraz, Iran
4 Department of Environmental Sciences, Gorgan University of Agricultural Sciences and Natural Resources, Gorgan, Iran
5 Department of Horticulture and Landscape Architecture, Oklahoma State University, Stillwater, USA

*Corresponding author's email: s.esmaeili@scu.ac.ir, hsalehi@shirazu.ac.ir

ARTICLE INFO

Article history:

Received: 27 July 2024,
Received in revised form: 3 October 2024,
Accepted: 12 October 2024

Article type:

Research paper

Keywords:

Distribution,
GIS,
MaxEnt model,
Native turfgrass,
Precipitation

ABSTRACT

Native turfgrasses and regionally adapted plants offer significant economic value while enriching genetic diversity. Habitat suitability modeling for these economically important species provides landscape managers with crucial tools for making informed decisions. These species are economically beneficial due to their roles in providing animal feed as forage, their use in landscape design as turf, erosion prevention, and their low water requirements, making them particularly valuable in areas facing water scarcity. In this study, species occurrence data were divided into training sets (75% of the total records) for model calibration and test sets (25% of the records) for evaluation. Accuracy was measured by the mean AUC values, with *L. perenne* achieving 0.94 and *L. rigidum* 0.84, indicating that the models performed better than random predictions. The model for *L. perenne* showed very good accuracy, while the model for *L. rigidum* demonstrated good accuracy. The habitat suitability for *L. perenne* was strongly influenced by factors such as annual average precipitation, elevation, sand content, river proximity, and salinity levels. In contrast, *L. rigidum*'s potential distribution was primarily affected by land use, sand content, annual average precipitation, and pH. Notably, *L. rigidum* demonstrated a wider range of suitability compared to *L. perenne*, indicating that it is more adaptable to regions where water is scarce or unevenly distributed, and where annual precipitation is low. In conclusion, *L. rigidum* showed greater resilience in areas with limited water resources, making it a better option for arid or semi-arid regions. These findings can help guide the selection of species for sustainable landscape management in different environmental conditions.

Introduction

In agriculture and natural resource management, sustainability focuses on optimizing the use of plant, animal, soil, and water resources while minimizing environmental damage. Key environmental factors, including geomorphology, climate, soil properties, land use, and biological interactions, significantly influence plant species distribution (Abolmaali et al., 2018). Advanced techniques such as Maximum Entropy Distribution (MaxEnt) modeling and geographic information systems (GIS) have been widely used for conserving endangered species, controlling invasive plants, and identifying suitable areas for plant cultivation (De Cauwer et al., 2014; Yu et al., 2014; Huang et al., 2020). Predicting suitable habitat distribution is essential for protecting rare or endangered species by identifying optimal conservation areas.

While climate change impacts species' distribution at a regional level, local factors like topography (e.g., slopes, aspects, elevations) are critical for determining species presence in specific areas (Breebaart et al., 2001; Wohlfahrt et al., 2008; Colgan et al., 2012; Farashi and Karimian, 2021). The distribution of grass species across different landscapes is also affected by a combination of biotic, abiotic, and human-induced factors (Hannaway et al., 2005; Groom and Harris, 2010).

Suitability mapping has been used to model the distribution of various forage and grass species, including *Lolium perenne* L., *Dactylis glomerata* L., and *Lolium arundinacea* (Schreb.) Darbysh. in the US and China (Hannaway et al., 2005, 2009). These studies incorporated climatic, topographic, and soil layers along with species tolerance characteristics. Similarly, Otunga et al. (2018) used topographic variables and logistic regression to predict the distribution of *Festuca* species in tropical montane areas, finding that elevation and slope were the most important factors.

The MaxEnt model has been employed to predict the distribution of narrowleaf plants such as *Leymus chinensis* (Chen et al., 2019), *Stipa* species (Yang et al., 2013), *Carex lasiocarpa* (Liu et al., 2018), *Festuca ovina* L. (Ghafari et al., 2020), and *Avena sativa* L. (Qin et al., 2023). It has also been applied to broadleaf species like Cornus officinalis (Cao et al., 2016), *Daphne mucronata* (Abolmaali et al., 2018), and *Rosa arabica* Crép. (Abdelaal et al., 2019). These examples highlight the value of MaxEnt and GIS in predicting species distribution for conservation and land-use planning.

Cao et al. (2016) studied the habitat distribution of *Cornus officinalis* using MaxEnt modeling and fuzzy logic, revealing that climatic factors were the most important for its growth, followed by soil and topography. Similarly, Abolmaali et al. (2018) predicted the habitat suitability of *Daphne mucronata* using MaxEnt in central Iran, while Abdelaal et al. (2019) used the MaxEnt model to project the current and future distributions of *Rosa arabica* in Egypt, identifying temperature, precipitation, and elevation as key factors. Chen et al. (2019) applied MaxEnt to evaluate the climatic suitability of *Leymus chinensis* in China, and Rahimian Boogar et al. (2019) found that temperature extremes were crucial variables in habitat modeling for *Juniperus*. Farashi and Karimian (2021) extended these methods to predict the distribution of *Agropyron cristatum*, *A. desertorum*, and *Festuca arundinacea* in Iran under current and future climates.

Among the grass species, *Lolium perenne* stands out as one of the most important forage and turf grasses in temperate regions due to its high digestibility, balanced seasonal dry matter production, and adaptability to various growing conditions (McDonagh et al., 2016; Capstaff and Miller, 2018). *Lolium rigidum* is similarly valued for its resistance to environmental stresses and compatibility with diverse ecological conditions (Oshib Nataj et al., 2012). Both species are significant for pasture and turf uses and are impacted by environmental and ecological factors.

Mapping suitable habitats for *L. perenne* and *L. rigidum* is essential for optimizing their growth and reducing costs related to establishment and management. Identifying suitable areas also helps expand artificial pastures and improve management of parks and green spaces. Given the variability in climatic and soil characteristics across different regions, this study aimed to identify the suitable habitats for these two species in Fars Province, Iran, and determine the factors influencing their distribution.

Previous research has focused on the habitat suitability of *Festuca* species; however, this study shifts the focus to *Lolium* species, particularly in relation to their environmental requirements and distribution range. Understanding these variables will enable better management decisions and contribute to the sustainable development of these valuable grass species.

Material and Methods

Study area

The study area is located in southern Iran (Fars Province, 31°40′–27°2′ N, 50°36′–55°34′ E) with a total area of approximately 122,608 km^2 (Fig. 1).

An extensive field study was conducted across Fars Province during 2016-2017 to collect *Lolium* samples, along with their corresponding soil samples from a depth of 30 cm. In total, 43 occurrence records for *L. perenne* and 131 locations for *L. rigidum* were documented using GPS (Garmin 62s model). Figure 1 presents the spatial distribution of these species across the region. All collected samples were then transferred to the greenhouse at the Horticultural Science Department, Shiraz University, for further analysis.

For taxonomic confirmation, one sample from each species was dried, labeled, and transferred to the herbarium of the Biology Department at Shiraz University for identification. The plant species identification was conducted by Prof. A.R.

Khosravi, a specialist at Shiraz University. The latitude and longitude coordinates of each occurrence record were organized in an Excel database, which served as the foundation for building the MaxEnt habitat suitability model.

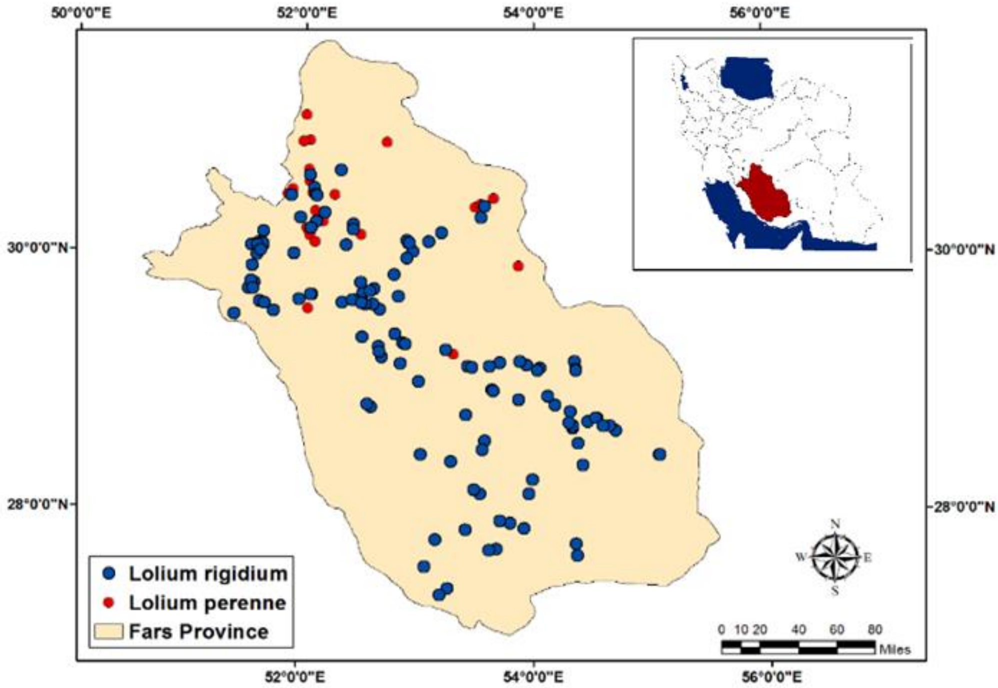

Fig. 1. The location of the presence species of *L. perenne* and *L. rigidum* in Fars province.

Data collection

For suitability mapping of *L. perenne* and *L. rigidum*, various environmental and soil parameters were required from each species' growing location. Soil texture (percentages of sand, silt, and clay), pH, and electrical conductivity (EC) were considered critical soil variables. Soil samples were collected at a depth of 0-30 cm from all recorded locations. These samples were dried at room temperature for 48 hours, followed by crushing and passing through two mesh sieves for further analysis. Soil texture was determined according to the method by Gee and Bauder (1986). The pH values of the soil samples were measured using the method described by Thomas (1996). Electrical conductivity (EC) was analyzed based on Rhoades' (1996) procedure.

Soil variable layers

To create the soil variable layers for Fars Province, soil data were collected from the Soil Science Department of Shiraz University and the Natural Resources of Fars Province. Since the soil map for this large region is incomplete, available data were used for the preparation of soil character layers, including percentages of clay, silt, and sand, as well as pH and EC. The geographic coordinate system was standardized as UTM. Using the Thiessen method in ArcGIS 10.2.2 (2014), soil character layers were generated for each variable. These layers were prepared with consistent parameters, including a cell size of 90 meters, same extent, dimension, and projection (in decimal degrees). All layers were converted to ASCII format for uploading into MaxEnt software version 3.3.3 (Fig. S1).

Climate layers

For climate data, daily precipitation data was sourced from the Fars Meteorological and Ministerial Power Stations. The annual precipitation mean, calculated from October 1986 to September 2017, was obtained for 189 stations across the province. To ensure normality, the data were normalized using the Johnson transformation method in Minitab 17 Statistical Software. The Kriging method was employed for spatial interpolation of the transformed data (Fig. S2). In addition, average January minimum and July maximum temperatures from 2001 to 2017 were calculated using data from 179 stations and interpolated using the Inverse Distance Weighting (IDW) method.

Topographic layers
SRTM DEM 90 m was downloaded from https://earthexplorer.usgs.gov/website (accessed on 1 July 2018). The slope (%) and aspect layers were made of DEM 90 m (Fig. S3).

Hydrology layers
The distance of the river was created based on the map of rivers in Arc GIS 10.2.2, and the topographic wetness index (TWI) was created in SAGA GIS 3. software based on the ASCII format of the DEM layer (Fig. S4).

Ground layers
Land use and distance of roads were obtained from the Natural Resources Organization in Fars province. Then these layers were created using ArcGIS 10.2.2 with the same cell size (90 m), extent, dimension, and projection for Fars province (Fig. S5).

Suitable habitat modeling procedure
Species occurrence data were systematically divided into training and testing sets to facilitate the modeling process. Specifically, 75% of the total occurrence records were allocated for model calibration (training set), while the remaining 25% were reserved for model evaluation (test set). During the modeling process, linear, quadratic, and hinge features were selected to capture the relationships between the species and their environmental variables effectively.

The produced model's performance was assessed by calculating the area under the curve (AUC) of the receiver operating characteristic (ROC) plot, as described by Phillips et al. (2006). The AUC is a crucial measure of model performance, ranging from 0 to 1, where a value of 1 signifies perfect discrimination between presence and absence (Fielding and Bell, 1997).

To evaluate the importance of various environmental variables in the model, the jackknife procedure was employed, following the methodology outlined by Yang et al. (2013). This technique assesses the training gain of each variable when run in isolation compared to the training gain when all variables are included, thus providing insights into which variables significantly influence habitat suitability.

Species response curves were generated to explore the relationships between habitat suitability and environmental variables for the target species. The final distribution model was based on the average logistic outputs from 15 replicated runs, allowing for a robust estimate of the probability of presence ranging from 0 (unlikely to occur) to 1 (most likely to occur) (Phillips et al., 2006).

The potential distribution maps produced exhibited values between 0 and 1, which were then categorized into four classes of potential habitats: High potential (>0.6), good potential (0.4-0.6), moderate potential (0.2-0.4), and low potential (<0.2). This classification, adapted from Yang et al. (2013), aids in understanding the suitability of different habitats for *L. perenne* and *L. rigidum*.

Results
For removing highly correlated variables, Pearson’s correlation was carried out among 15 ASCII raster variables in R software 3.5.1. before the performance of the MaxEnt model. Results of the Pearson correlation are presented in Table 1. Based on these results, between two highly correlated variables (>0.7), a more important parameter was selected for building the MaxEnt model. Thus, the January minimum temperature, the July maximum temperature, and the silt percentage were removed from the MaxEnt model. In addition, we also removed the distance of the road parameter to avoid error results in the MaxEnt model. Based on this, we used 11 parameters for the performance of the MaxEnt model.

The mean AUC values of the training data for *L. perenne* and *L. rigidum* were 0.94 and 0.84, respectively, indicating that the model performed with excellent and good accuracy (Fig. 2).

According to obtained results from the MaxEnt model for *L. perenne*, five variables, including the annual average precipitation (Bio_10), DEM (Bio_6), sand percentage (Bio_9), distance of the river (Bio_2), and EC (Bio_1), had more than 85% contribution to the model. Annual average precipitation (Bio_10) explained 29.4% of the total variance and was thus identified as the main factor affecting the spatial distribution of *L. perenne* (Table 2).

In *L. rigidum*, four variables, including land use (Bio_15), sand percentage (Bio_9), annual average precipitation (Bio_10), and acidity or pH (Bio_5), had a combined contribution of more than 85% to the model. The most important factor that affects the spatial distribution of *L. rigidum* belongs to land use, with 42.5% in Fars Province (Table 3).

In addition, the jackknife test revealed that *L. perenne*'s distribution was largely affected by annual average precipitation (Bio_10), DEM (Bio_6), sand percentage (Bio_9), distance from the river (Bio_2), and EC (Bio_1). The potential distribution of *L. rigidum* in Fars Province was more affected by land use (Bio_15), sand (Bio_9), annual average precipitation (Bio_10), and pH (Bio_5) (Fig. 3).

Table 1. Correlation matrix among ASCII raster's variables with Pearson test using R software.

	Bio_1	Bio_2	Bio_3	Bio_4	Bio_5	Bio_6	Bio_7	Bio_8	Bio_9	Bio_10	Bio_11	Bio_12	Bio_13	Bio_14	Bio_15
Bio_1	1.00														
Bio_2	0.06	1.00													
Bio_3	0.13	−0.16	1.00												
Bio_4	0.12	−0.09	0.78	1.00											
Bio_5	0.06	0.00	−0.04	0.04	1.00										
Bio_6	−0.14	0.16	−0.86	−0.70	0.08	1.00									
Bio_7	0.10	0.06	−0.17	−0.06	0.26	0.16	1.00								
Bio_8	0.07	0.09	−0.25	−0.24	−0.03	0.20	0.28	1.00							
Bio_9	−0.09	−0.09	0.23	0.15	−0.19	−0.20	−0.89	−0.64	1.00						
Bio_10	−0.08	0.00	−0.29	−0.19	−0.11	0.25	0.10	0.19	−0.16	1.00					
Bio_11	−0.03	0.06	0.02	0.00	−0.05	0.17	−0.05	−0.04	0.06	0.15	1.00				
Bio_12	−0.01	−0.01	0.01	0.03	0.01	−0.02	0.01	0.00	−0.01	0.03	−0.03	1.00			
Bio_13	0.03	−0.01	−0.07	−0.01	0.04	−0.11	0.05	0.07	−0.07	−0.09	−0.53	0.02	1.00		
Bio_14	0.01	−0.04	0.23	0.14	−0.02	−0.19	−0.06	−0.06	0.07	−0.28	0.07	0.01	−0.10	1.00	
Bio_15	0.03	0.12	0.03	0.05	−0.05	−0.06	−0.02	0.07	−0.01	0.14	−0.06	0.02	0.12	−0.09	1.00

Bio_1 = EC (dS m^{-1}). Bio_2 = Distance of river (m). Bio_3 = January minimum temperature. Bio_4 = July maxi mum temperature. Bio_5 = pH. Bio_6 = DEM. Bio_7 = Soil silt (%). Bio_8 = Soil clay (%). Bio_9 = Soil sand (%). Bio_10 = Annual average precipitation (mm). Bio_11 = Slope (%). Bio_12 = Aspect. Bio_13 = Topographic Wetness Index. Bio_14 = Distance of road (m). Bio_15 = Land use.

Table 2. The variables used in the *L. perenne* distribution modeling process.

Variable Code	Variable	Percent Contribution	Permutation Importance
Bio_1	EC (dS m^{-1})	5.2	4.1
Bio_2	Distance of river (m)	5.9	7.6
Bio_5	pH	0.5	0.2
Bio_6	DEM	27.2	51
Bio_8	Clay (%)	0.9	0.9
Bio_9	Sand (%)	18.7	19.6
Bio_10	Annual average precipitation (mm)	29.4	9.4
Bio_11	Slope (%)	2.7	3
Bio_12	Aspect	3.7	1
Bio_13	Topographic Wetness Index (TWI)	0.8	0.8
Bio_15	Land use	5	2.4

Table 3. The variables used in the *L. rigidum* distribution modeling process.

Variable Code	Variable	Percent Contribution	Permutation Importance
Bio_1	EC (dS m^{-1})	1.5	0.8
Bio_2	Distance of river (m)	0.4	0.7
Bio_5	pH	5.1	1.8
Bio_6	DEM	4.6	6.7
Bio_8	Clay (%)	1	4.2
Bio_9	Sand (%)	25.3	31.9
Bio_10	Annual average precipitation (mm)	13.7	24.7
Bio_11	Slope (%)	2.7	3
Bio_12	Aspect	3.7	9.9
Bio_13	Topographic Wetness Index (TWI)	1	1.2
Bio_15	Land use	42.5	16.1

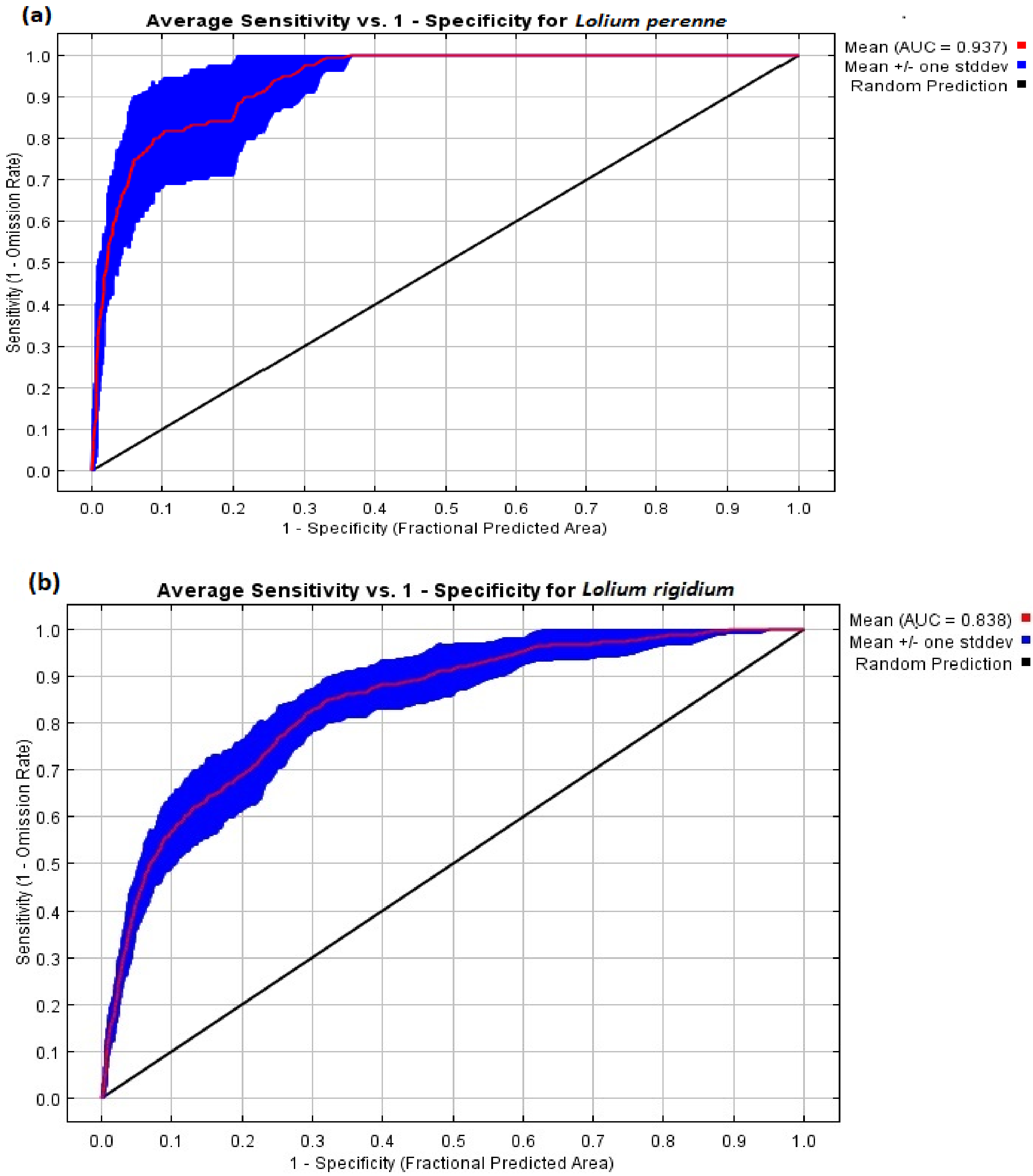

Fig. 2. The receiver operating characteristic (ROC) curve generated in MaxEnt shows an average of 15 repetitions of the model and standard deviations. The average test AUC for the 15 replicate runs is 0.937 and 0.840 for *L. perenne* (a) and *L. rigidum* (b), and the dark blue range shows the mean of the standard deviation is 0.029 (a) and 0.027 (b).

Species response curves indicate the relationships between variables and the species occurrence probability. They demonstrate biological tolerances and habitat preferences for target species. According to the obtained response curves of the species, *L. perenne* prefers habitats with annual average precipitation of 550 to 720 mm, elevations of 1500–2300 mm above sea level, light soil texture (40 to 65% sand), besides rivers (distance nearest to river), and salinity less than 4 ds m^{-1} (Figs. 4a-e).

Based on response curves, results for *L. rigidum* showed that urban, dry farming, and irrigated farming are suitable habitats for this species. In the other world, light soil texture (sand percentage greater than 20%) and an annual average precipitation of 280–600 mm prevails (Figs. 5a-c). Species distribution maps showed that about 7.1% and 4.82% of the study area were recognized as high-potential habitats of *L. perenne* and *L. rigidum* in the current condition, respectively (Table 4 and Figs. 6a, b).

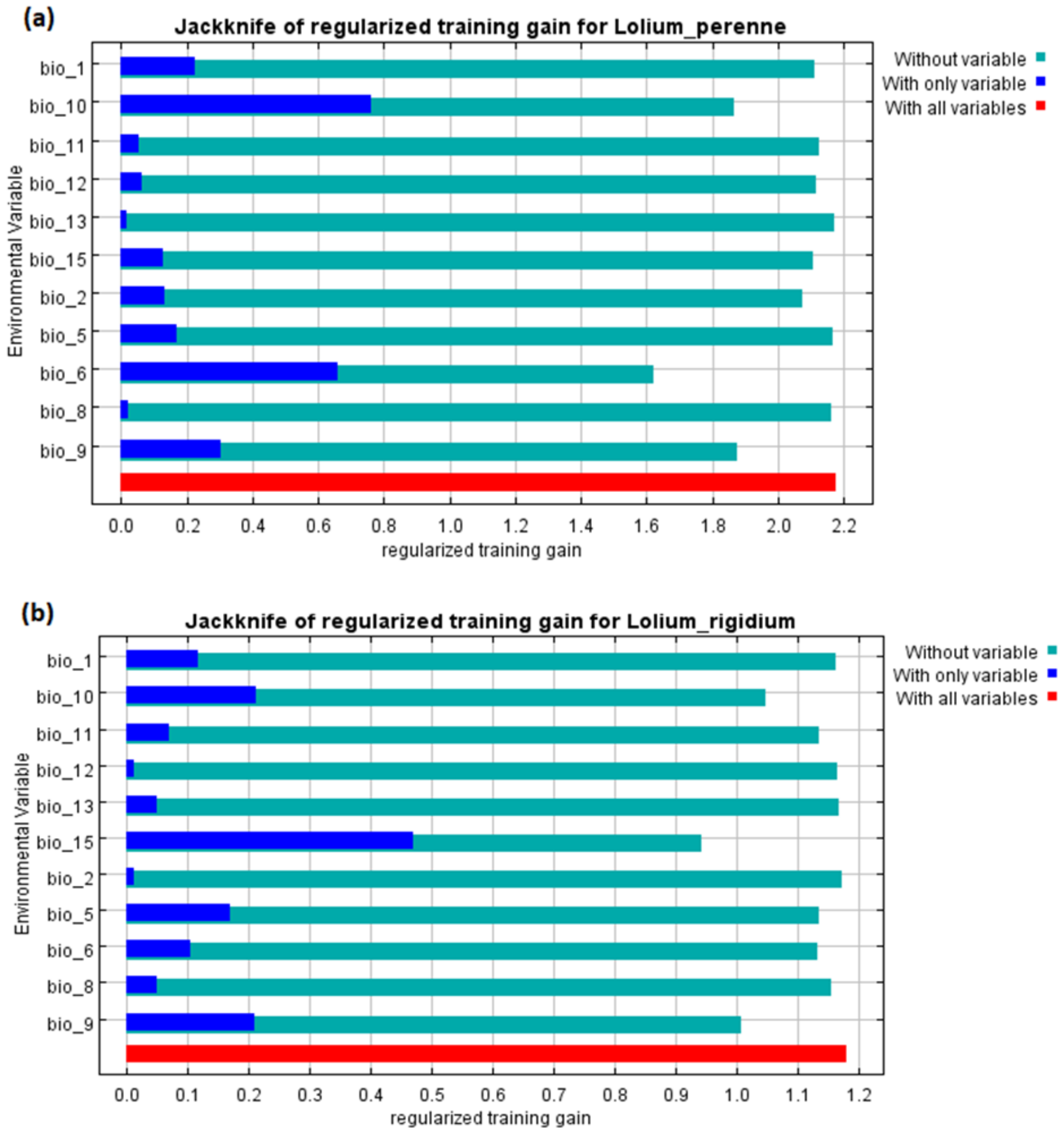

Fig. 3. Relative predictive power of different environmental variables based on the jackknife of regularized training gain in MaxEnt models for (a) *L. perenne* and (b) *L. rigidum*. Bio_1 = EC (dS m^{-1}). Bio_2 = Distance of river (m). Bio_3 = January minimum temperature. Bio_4 = July maximum temperature. Bio_5 = pH. Bio_6 = DEM. Bio_7 = Soil silt (%). Bio_8 = Soil clay (%). Bio_9 = Soil sand (%). Bio_10 = Annual average precipitation (mm). Bio_11 = Slope (%). Bio_12 = Aspect. Bio_13 = Topographic Wetness Index. Bio_14 = Distance of road (m). Bio_15 = Land use.

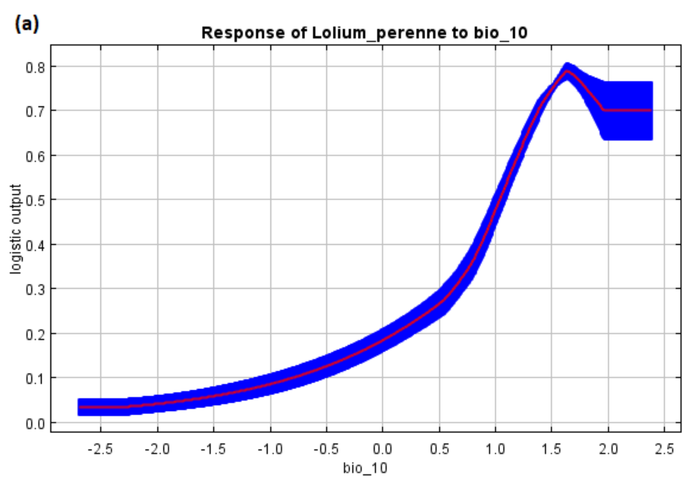

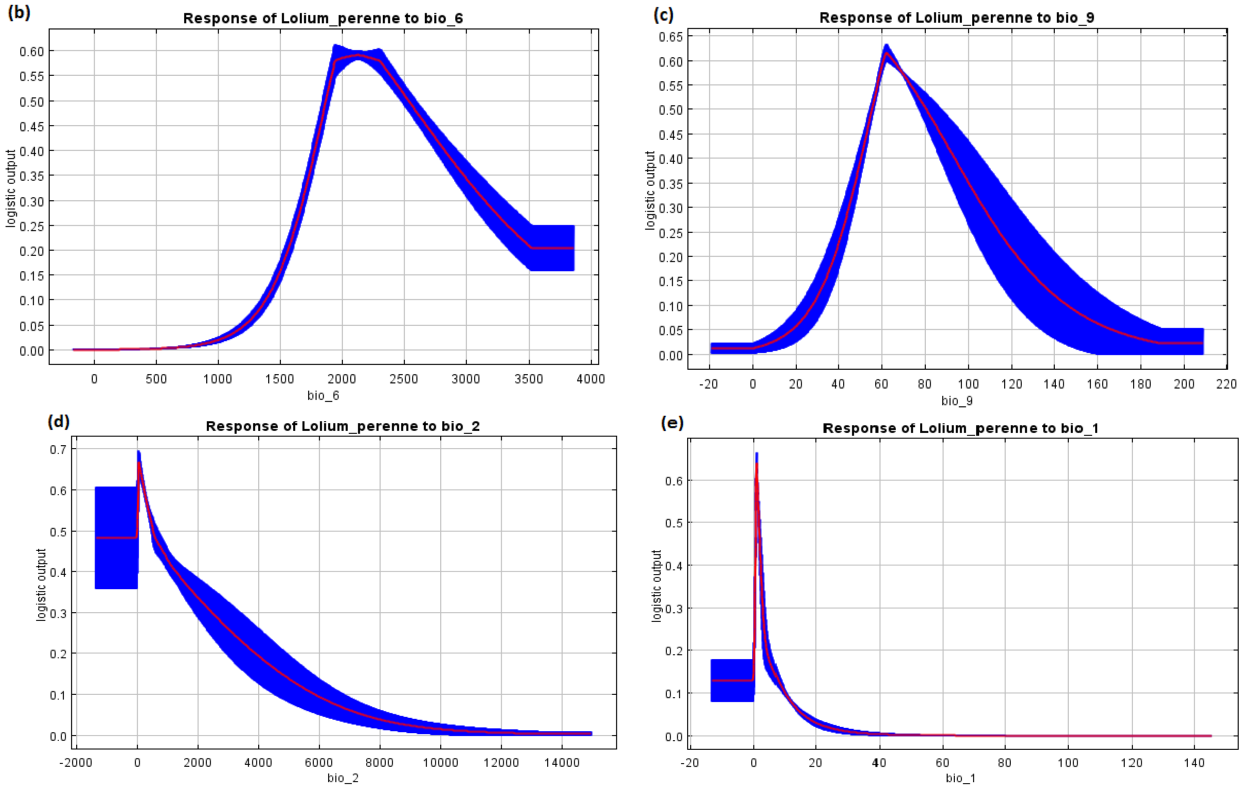

Fig. 4. *L. perenne* response curves concerning (a) annual average precipitation (Bio_10), (b) DEM (Bio_6), (c) soil sand percentage (Bio_9), (d) distance of rivers (Bio_2), and (e) EC (Bio_1). Red lines show how the logistic prediction changed as each environmental variable was varied while keeping all other variables at their average sample value; the blue color represents the mean ± one standard deviation.

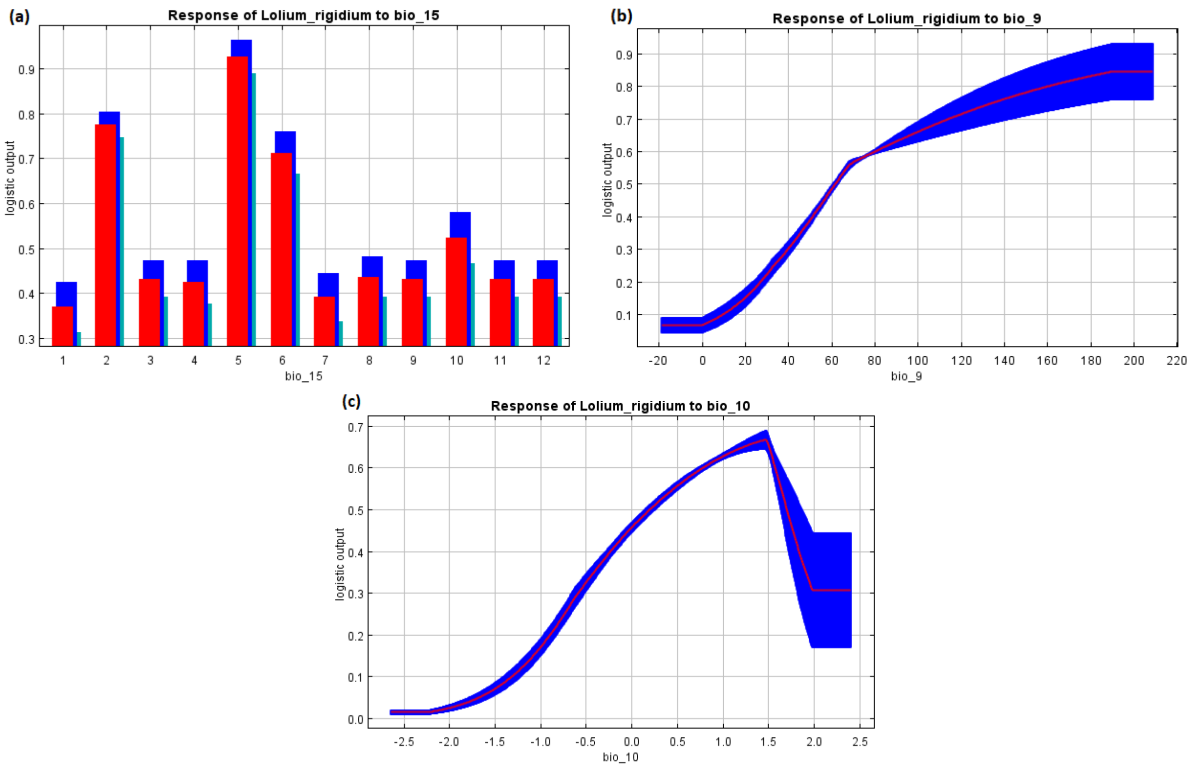

Fig. 5. *L. rigidum* response curves concerning (a) land use (Bio_15), (b) soil sand percentage (Bio_9), and (c) annual average precipitation (Bio_10). Red lines show how the logistic prediction changed as each environmental variable was varied while keeping all other variables at their average sample value; the blue color represents the mean ± one standard deviation.

Discussion

Most research on habitat suitability using the MaxEnt model has relied on bioclimatic maps from global climate databases. In this study, we utilized ground data to create ASCII raster variables. There is limited information regarding the spatial distribution and habitat suitability of turfgrasses in Iran and globally, particularly in relation to the MaxEnt model.

Table 4. The areas of each potential habitat class using MaxEnt under current conditions in Fars province.

Habitat Suitability Classes	Area Percent	
	L. perenne	*L. rigidum*
Least potential (<0.2)	80.1	58.4
Moderate potential (0.2–0.4)	0.004	22.56
Good potential (0.4–0.6)	12.88	14.16
High potential (>0.6)	7.06	4.82

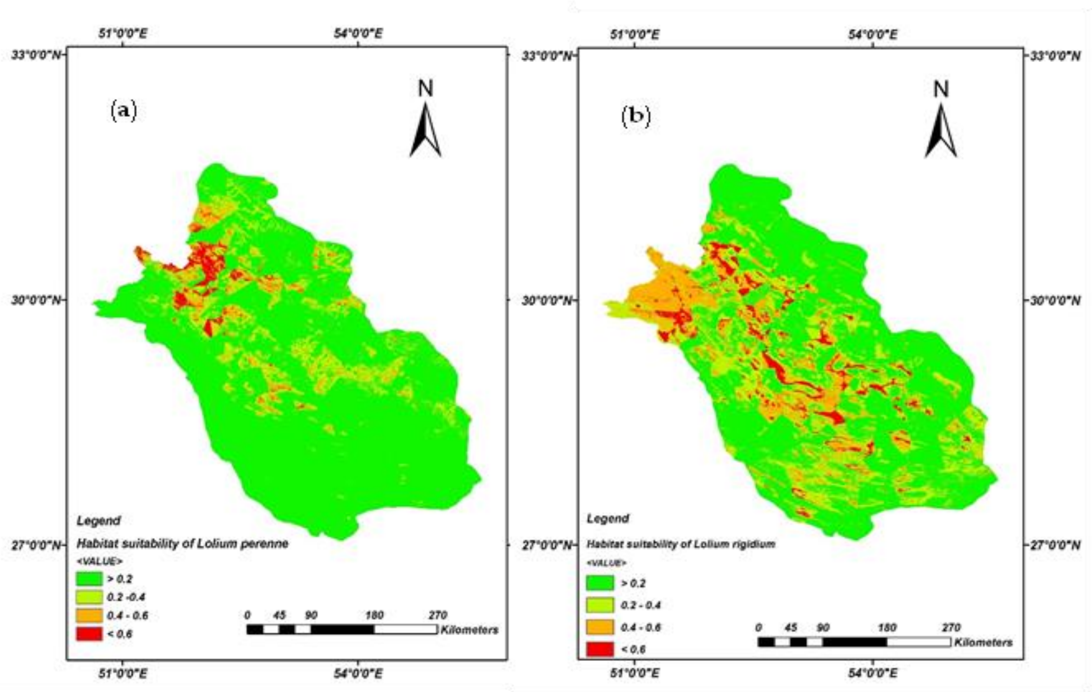

Fig. 6. Habitat suitability potential mapping of *L. perenne* (a) and *L. rigidum* (b) in Fars province.

In a previous study by Otunga et al. (2018), the distribution of *Festuca* species was examined in a sub-tropical area (Fort Nottingham) using GIS and binary logistic regression. Their findings indicated that these species thrived at elevations between 1,669.90 and 1,762.47 meters and on slopes ranging from 0° to 24.99°. Notably, *Festuca* species were more prevalent on higher northern slopes compared to southern slopes.

More recently, Ghafari et al. (2020) assessed the habitat suitability distribution of *Festuca ovina* along the altitude gradient in the Moghan-Sabalanestan rangelands of Ardabil, employing the MaxEnt model. Their results identified elevation, slope, patch size, potassium concentration (at 15–30 cm depth), and lime content (at 0–15 cm depth) as the most significant contributors to the model. The area under the curve (AUC) was 0.86, indicating a high accuracy and efficiency of the model in pinpointing the most suitable distribution areas. The highest occurrences of *Festuca ovina* were found at an altitude of 2,500 meters. In contrast, increases in potassium (15–30 cm depth) and lime (0–15 cm depth) significantly decreased the likelihood of the species' presence. The maximum probability of occurrence was observed in areas where potassium levels were less than 17 m Eq L^{-1}, lime levels were below 2%, and slope gradients were between 30% and 50%.

Generally, plant species distribution is closely associated with precipitation levels. Recent studies have shown that both precipitation and elevation play crucial roles in the distribution of *Daphne mucronate* in central Iran, particularly in Isfahan Province (Abolmaali et al., 2018). In our study, a significant contribution of annual average precipitation to the distribution of *Lolium perenne* was also noted. This species was predominantly found in the northern regions of Fars Province, where the annual average precipitation ranges from 450 to 700 mm. Alongside precipitation, elevation and the sand percentage in the top 0–30 cm of soil also emerged as critical determinants of habitat suitability for *Lolium perenne* (see Table 2 and Figures 4a-d).

Autecological studies of *Lolium rigidum* and *Lolium perenne* were conducted in Mazandaran, a northern province of Iran (Oshib Nataj et al., 2011, 2012). The researchers found that relative humidity significantly influenced the presence and frequency of *L. perenne*. They reported that this species is more abundant in very humid to humid climates—characterized by a higher Dumarten aridity index—compared to Mediterranean and semi-arid habitats with lower Dumarten indices. Additionally, they observed that annual average precipitation and evaporation had minimal impact on the abundance of *L. perenne* in Mazandaran's habitats (Oshib Nataj et al., 2011). These conflicting findings may stem from variations in methodology, climate, soil conditions, and geographical locations.

The study also noted that both species are present across various sites, ranging from −22 meters to 1,700 meters above sea level. *L. perenne* is more prevalent in lowland areas than in upland regions. Specifically, the occurrence of *L. perenne* declines at altitudes above 2,300 meters and disappears entirely above 3,800 meters (Fig. 4b). Guo et al. (2019) identified four major climatic factors affecting the distribution of perennial cultivated grasses in the Northwest Sichuan Plateau: the wet index, accumulated temperature, isotherm, and annual average temperature range. Furthermore, elevation is a significant topographic factor influencing species distribution (Otunga et al., 2018; Ghafari et al., 2020; Boral and Moktan, 2021).

Similar to the previous findings (Oshib Nataj et al., 2011), *L. perenne* is frequently found along riversides, irrigation channels, rocky areas, sandy hills, and agricultural fields. A species response curve illustrates the relationship between various environmental variables and the probability of occurrence, highlighting the ecological tolerances and habitat preferences of each species. The model response curve (Fig. 4c) indicates that *L. perenne* is most suited to light-textured soils containing 40–65% sand in the top 0–30 cm layer. The response curve for *L. rigidum* (Fig. 5b) reveals that its suitability increases with sand percentages exceeding 20% in the same soil depth.

According to the literature (Oshib Nataj et al., 2011, 2012; Xu et al., 2020), both species exhibit strong adaptability and can thrive in a wide range of soil types. These findings align with previous studies demonstrating that variations in soil characteristics significantly influence the presence, distribution, and abundance of vegetation species (Raich et al., 2000; Jafari et al., 2004).

In some studies, river distance has been identified as a crucial variable in MaxEnt modeling for plant species, such as *Homonoia riparia* Lour (Yi et al., 2016). The results from the Jackknife test demonstrated that river distance plays a significant role in the habitat suitability distribution of *L. perenne*. In natural habitats, *L. perenne* is known to favor wet, sandy soils and tends to grow more abundantly along riverbanks. These observations align with reports by Oshib Nataj et al. (2011).

Yi et al. (2016) predicted the habitat suitability for the medicinal plant *H. riparia* using the MaxEnt model, identifying average annual temperature as the most critical variable influencing its distribution. The most suitable habitats were found in the warmer regions of Yunnan Province, China. Their findings also indicated that suitable habitats are primarily located along rivers, with habitat suitability decreasing as the distance from the river increases. This pattern is consistent with the preference response curve observed for *L. perenne* (Fig. 4d).

Another study investigated the habitat suitability distribution of *F. arundinacea* using MaxEnt and logistic regression composite models, revealing that climate factors (particularly temperature and rainfall), topography (elevation and aspect), and land use (such as farming) significantly affected the species' occurrence. The composite model indicated that lower temperatures, more southerly slopes, and less residential land use were associated with higher occurrences of tall fescue (Lemke and Brown, 2012).

As shown in Table 3 and Fig. 5b, land use emerged as the dominant variable influencing the habitat suitability distribution of *L. rigidum* in Fars Province. This species was found to thrive primarily in urban and dry farming regions. Previous studies have also highlighted that land use impacts the diversity, distribution, and abundance of vegetation species in pastures and grasslands (O'Connor, 2005).

In our study, the area under the curve (AUC) values for *L. perenne* and *L. rigidum* were 0.937 and 0.84, respectively. These values are comparable to those reported in earlier studies on various species, such as *Perilla frutescens* in Uttarakhand (0.915; Sharma et al., 2018), *Boswellia serrata* in India (0.938; Rajpoot et al., 2020), and *Rhododendron arboreum* in Uttarakhand (0.886; Bhandari et al., 2020). A recent study by Purohit and Rawat (2022) utilized the MaxEnt model to predict the distribution of *Clerodendrum infortunatum* L. under current climatic conditions and for future scenarios. Their results indicated that the MaxEnt model was accurate, achieving an AUC of 0.837, with rainfall from the coldest section and elevation as the main influencing factors.

In a subsequent study, Farashi and Karimian (2021) demonstrated that the MaxEnt model exhibited the highest true skill statistics (TSS) and AUC values for *Agropyron desertorum*, *Agropyron cristatum*, and random forest analyses for *F. arundinacea* in both current and future scenarios. Their findings indicated that annual average precipitation, as well as the average temperatures of the warmest and coldest quarters, and geological factors significantly influenced the modeling of potential distributions for all species. Both *A. desertorum* and *F. arundinacea* showed increased habitat suitability in response to rising precipitation levels. Specifically, they noted that higher annual precipitation enhanced habitat suitability for both species, while increases in the mean temperatures of the coldest and warmest quarters reduced it.

Similarly, Liu et al. (2018) estimated the distribution patterns of *Carex lasiocarpa* under historical and future climate scenarios by simulating the main climatic factors affecting its distribution. Additionally, Qin et al. (2023) found that the distribution of the cereal crop *Avena sativa* L. was significantly influenced by seasonal precipitation, altitude, and seasonal temperature, as determined by the MaxEnt model. They reported that *Avena sativa* thrives in regions with the wettest monthly precipitation ranging from 3 to 38 mm, an annual mean temperature between 7.5 and 25.8 °C, and the driest seasonal precipitation ranging from 0 to 30 mm. These conditions align with the species' characteristics of cold weather tolerance and drought resistance. Furthermore, they indicated that *Avena sativa* is likely to shift to higher altitudes and latitudes in response to climate changes, with this shift being more pronounced under high radiative forcing scenarios. This transition may lead to a disconnect between the main production areas for *Avena sativa* and the regions with suitable climatic conditions.

Conclusions

Using MaxEnt modeling, we estimated and predicted the presence and potential habitat quality of *L. perenne* and *L. rigidum* in Fars Province. The model proved reasonable and accurate, as indicated by the evaluation results of the AUC index. Among the 11 variables selected for model construction, *L. perenne*'s habitat was primarily influenced by five key factors: annual average precipitation, elevation, soil sand percentage, distance from a river, and electrical conductivity. In contrast, the habitat suitability of *L. rigidum* was predominantly affected by land use, with sand percentage and annual average precipitation following as significant factors. Notably, *L. rigidum* exhibits a more extensive range of suitable areas compared to *L. perenne*. Our findings suggest that *L. rigidum* demonstrates greater tolerance in regions where water is scarce or unevenly distributed, as well as in areas receiving lower precipitation. This research has precisely identified suitable locations for these species and outlined the main environmental factors influencing their distribution. The data provided will support natural resource and landscape managers in determining optimal planting areas for these species, contributing to the restoration of pastures and green spaces in Fars Province and other regions with similar conditions.

Author contributions

HS project administration and supervision; SE investigation and writing; HS, MKK, SRFS, AMT, and MX, review and editing. All authors have read and agreed to the published version of the manuscript.

Funding

This research was funded by the Shiraz University Council for Research.

Conflict of Interest

The authors indicate no conflict of interest in this work.

References

Abdelaal M, Fois M, Fenu G, Bacchetta G. 2019. Using MaxEnt modeling to predict the potential distribution of the endemic plant Rosa arabica Crép. in Egypt. Ecological Informatics 50, 68-75.

Abolmaali SM-R, Tarkesh M, Bashari H. 2018. MaxEnt modeling for predicting suitable habitats and identifying the effects of climate change on a threatened species, Daphne mucronata, in central Iran. Ecological Informatics 43,116-123.

Bhandari MS, Meena RK, Shankhwar R, Shekhar C, Saxena J, Kant R, Pandey VV, Barthwal S, Pandey S, Chandra G. 2020. Prediction mapping through maxent modeling paves the way for the conservation of *Rhododendron arboreum* in Uttarakhand Himalayas. Journal of the Indian Society of Remote Sensing 48, 411-422.

Boral D, Moktan S. 2021. Predictive distribution modeling of Swertia bimaculata in Darjeeling-Sikkim Eastern Himalaya using MaxEnt: current and future scenarios. Ecological Processes 10, 26.

Breebaart J, Van De Par S, Kohlrausch A. 2001. Binaural processing model based on contralateral inhibition. I. Model structure. Journal of the Acoustical Society of America 110, 1074-1088.

Cao B, Bai C, Zhang L, Li G, Mao M. 2016. Modeling habitat distribution of Cornus officinalis with Maxent modeling and fuzzy logics in China. Journal of Plant Ecology 9,742-751.

Capstaff NM, Miller AJ (2018) Improving the yield and nutritional quality of forage crops. Frontiers in Plant Science 9:535.

Colgan MS, Baldeck CA, Féret J-B, Asner GP. 2012. Mapping savanna tree species at ecosystem scales using support vector machine classification and BRDF correction on airborne hyperspectral and LiDAR data. Remote Sensing 4, 3462-3480.

De Cauwer V, Muys B, Revermann R, Trabucco A. 2014. Potential, realised, future distribution and environmental suitability for *Pterocarpus angolensis* DC in southern Africa. Forest Ecology and Management 315, 211-226.

Farashi A, Karimian Z. 2021. Assessing climate change risks to the geographical distribution of grass species. Plant Signaling and Behavior 16, 1913311.

Fielding AH, Bell JF. 1997. A review of methods for the assessment of prediction errors in conservation presence/absence models. Environmental Conservation 24, 38-49.

Ghafari S, Ghorbani A, Moammeri M, Mostafazadeh R, Bidar Lord M, Kake Mami A. 2020. Modeling and determining effective factors in distribution of Festuca ovina using Maxent in rangelands of northern Ardabil province. Iranian Journal of Range and Desert Research 27, 433–462. https://doi.org/10.22092/ijrdr.2020.125233.1828. (In Persian).

Groom R, Harris S. 2010. Factors affecting the distribution patterns of zebra and wildebeest in a resource-stressed environment. African Journal of Ecology 48, 159-168.

Guo B, Wang S, Chen C, Wang M, Li T. 2019. Prediction of the Distribution of perennial cultivated grasses in the northwest Sichuan Plateau, China under climate change. Journal of Geoscience and Environment Protection 7, 95-111.

Hannaway DB, Daly C, Cao WX, Luo WH, Wei YR, Zhang WL, Xu AG, Lu CA, Shi XZ, Li XL. 2005. Forage species suitability mapping for China using topographic, climatic and soils spatial data and quantitative plant tolerances. Agricultural Sciences in China 4, 660.

Huang X, Ma L, Chen C, Zhou H, Yao B, Ma Z. 2020. Predicting the suitable geographical distribution of *Sinadoxa corydalifolia* under different climate change scenarios in the Three-River Region using the MaxEnt model. Plants 9, 1015.

Lee JM, Sathish P, Donaghy DJ, Roche JR. 2010. Plants modify biological processes to ensure survival following carbon depletion: a *Lolium perenne* model. PLoS One 5, e12306.

Lemke D, Brown JA. 2012. Habitat modeling of alien plant species at varying levels of occupancy. Forests 3, 799-817.

McDonagh J, O'Donovan M, McEvoy M, Gilliland T. 2016. Genetic gain in perennial ryegrass (*Lolium perenne*) varieties 1973 to 2013. Euphytica 212, 187-199.

O'connor T. 2005. Influence of land use on plant community composition and diversity in Highland Sourveld grassland in the southern Drakensberg, South Africa. Journal of Applied Ecology 42, 975-988.

Oshib Nataj M, Shekarchi H, Keshavarzi M, Akbarzadeh M. 2011. Autecology of *Lolium perenne* L. in Mazandaran province. Iranian Journal of Range and Desert Research 18, 90–106. https://doi.org/10.22092/ijrdr.2011.102010. (In Persian).

Oshib Nataj M, Shekarchi H, Akbarzadeh M, Keshavarzi M. 2012. An autecological study of Lolium rigidum L. in Mazandaran Province. Journal of Plant Biological Sciences 3, 37-46.

Otunga C, Odindi J, Mutanga O, Adjorlolo C, Botha J. 2018. Predicting the distribution of C3 (*Festuca* spp.) grass species using topographic variables and binary logistic regression model. Geocarto International 33, 489-504.

Phillips SJ, Anderson RP, Schapire RE. 2006. Maximum entropy modeling of species geographic distributions. Ecological Modelling 190, 231-259.

Purohit S, Rawat N. 2022. MaxEnt modeling to predict the current and future distribution of *Clerodendrum infortunatum* L. under climate change scenarios in Dehradun district, India. Modeling Earth Systems and Environment 8, 2051-2063.

Qin M, Gao X, Feng M, Jin N, Wang C, Cheng W. 2023. Modeling of the potential geographical distribution of naked oat under climate change. Frontiers in Plant Science 13, 1009577.

Rahimian Boogar A, Salehi H, Pourghasemi HR, Blaschke T. 2019. Predicting habitat suitability and conserving *Juniperus* spp. habitat using SVM and maximum entropy machine learning techniques. Water 11, 2049.

Raich JW, Tufekciogul A (2000) Vegetation and soil respiration: correlations and controls. Biogeochemistry 48, 71-90.

Rajpoot R, Adhikari D, Verma S, Saikia P, Kumar A, Grant KR, Dayanandan A, Kumar A, Khare PK, Khan ML. 2020. Climate models predict a divergent future for the medicinal tree *Boswellia serrata* Roxb. in India. Global Ecology and Conservation 23, e01040.

Rhoades J. 1996. Salinity: Electrical conductivity and total dissolved solids. Methods of soil analysis: Part 3 Chemical methods 5, 417-435.

Sharma S, Arunachalam K, Bhavsar D, Kala R. 2018. Modeling habitat suitability of Perilla frutescens with MaxEnt in Uttarakhand—A conservation approach. Journal of Applied Research on Medicinal and Aromatic Plants 10, 99-105.

Tallowin J, Rook A, Rutter S. 2005. Impact of grazing management on biodiversity of grasslands. Animal Science Journal 81, 193-198.

Thomas GW. 1996. Soil pH and soil acidity. Methods of soil analysis: part 3 chemical methods 5, 475-490.

Wohlfahrt G, Anderson-Dunn M, Bahn M, Balzarolo M, Berninger F, Campbell C, Carrara A, Cescatti A, Christensen T, Dore S. 2008. Biotic, abiotic, and management controls on the net ecosystem CO2 exchange of European mountain grassland ecosystems. Ecosystems 11, 1338-1351.

Yang XQ, Kushwaha S, Saran S, Xu J, Roy P. 2013. Maxent modeling for predicting the potential distribution of medicinal plant, *Justicia adhatoda* L. in Lesser Himalayan foothills. Ecological Engineering 51, 83-87.

Yu J, Wang C, Wan J, Han S, Wang Q, Nie S. 2014. A model-based method to evaluate the ability of nature reserves to protect endangered tree species in the context of climate change. Forest Ecology and Management 327, 48-54.

Supplemental

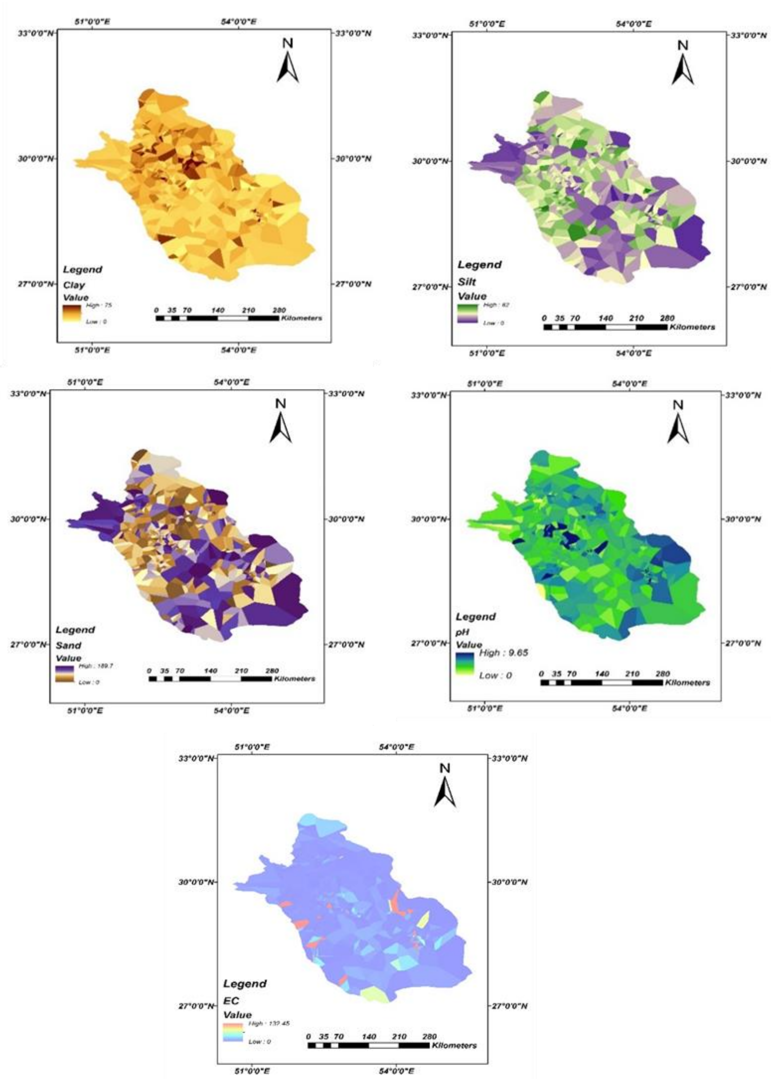

Figure S1. Soil clay, silt, and sand percentages, pH, and EC maps at a depth of 0–30 cm in Fars province.

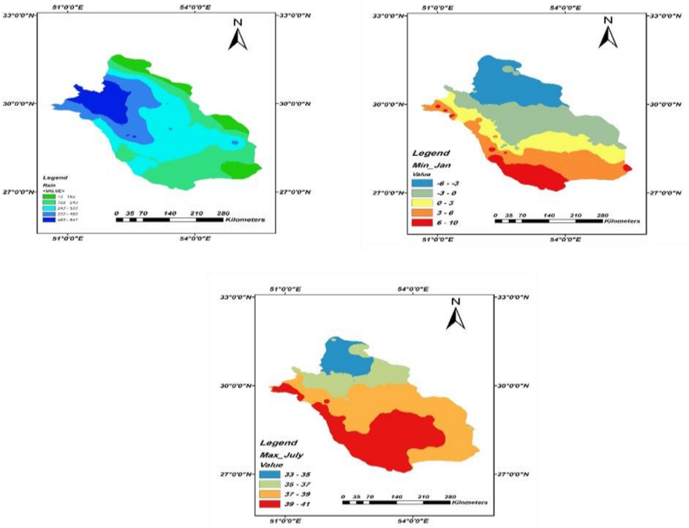

Figure S2. Maps of annual average precipitation and January minimum and July maximum temperatures in Fars province.

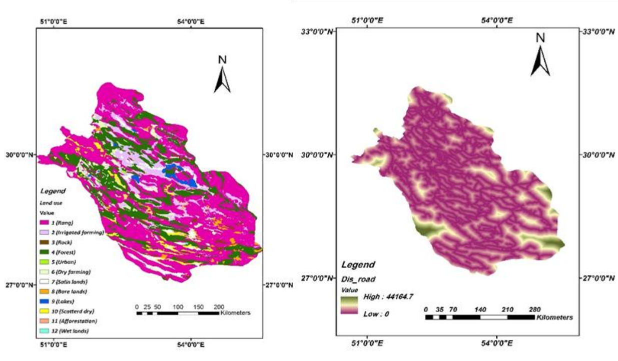

Figure S5. Land use and distance of road maps from Fars Province.

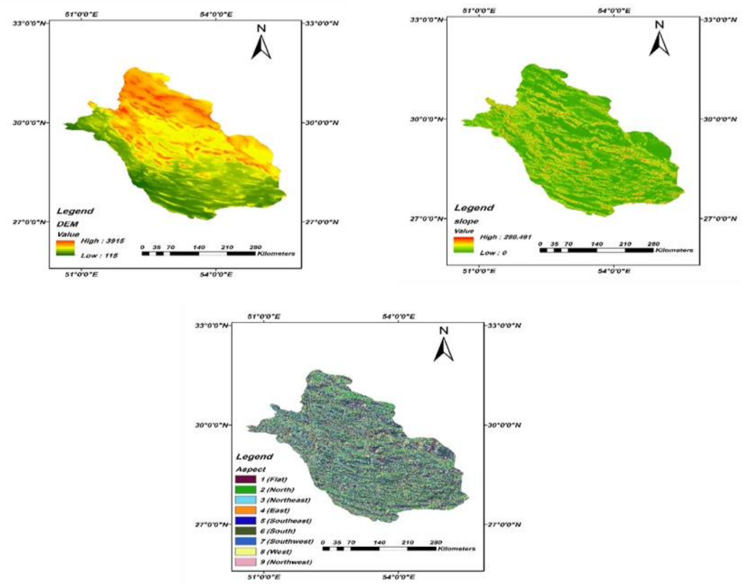

Figure S3. DEM, slope (%), and aspect maps of Fars province.

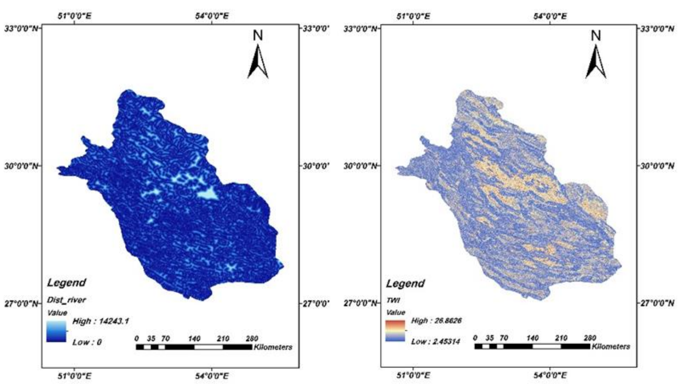

Figure S4. Distance of the river and topographic wetness index (TWI) maps from Fars province.